Mechanical and thermoelectric properties of $Ca_3Co_4O_9$ ceramics consolidated by SPS process

D. Kenfaui[1], G. Bonnefont[2], D. Chateigner[1], G. Fantozzi[2]
M. Gomina[1] and J.G. Noudem[1]

[1]Laboratoire CRISMAT, UMR 6508 CNRS / ENSICAEN
6, Boulevard Maréchal Juin, 14050 Caen Cedex 4
http://www-crismat.ensicaen.fr

[2]Laboratoire MATEIS- INSA, Bât. B. Pascal, 5° étage
7 avenue Jean Capelle 69621, Villeurbanne Cedex
http://mateis.insa-lyon.fr

XIth ECERS Conference, Krakow, Poland

June 21-25, 2009

Outline

- **Thermoelectric Materials**
  - **$Ca_3Co_4O_9$ Oxides**
  - **Material preparation**
- **Microstructure and texture analyses**
- **Thermoelectric characterizations**
  - **Electrical resistivity and Seebeck coefficient**
  - **Power factor**
- **Mechanical properties**
  - **Young's modulus and Hardness**
  - **Strength**
- **Conclusions and outlooks**

Thermoelectric effects

Heat ⟵ **Thermoelectrics** ⟶ Current

Peltier effect

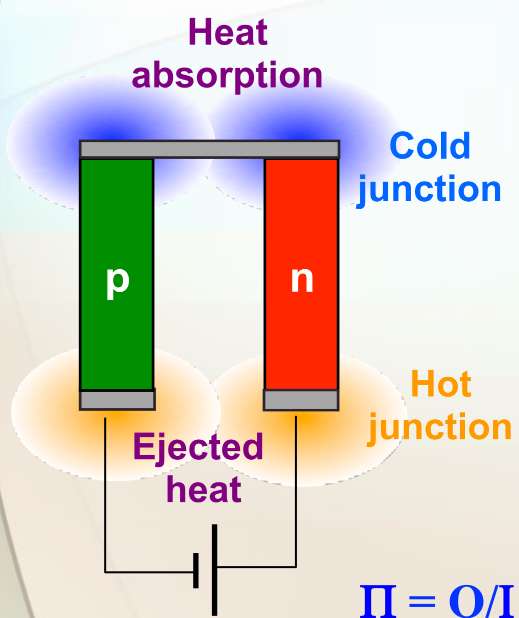

$\Pi = Q/I$

Refrigeration

Seebeck effect

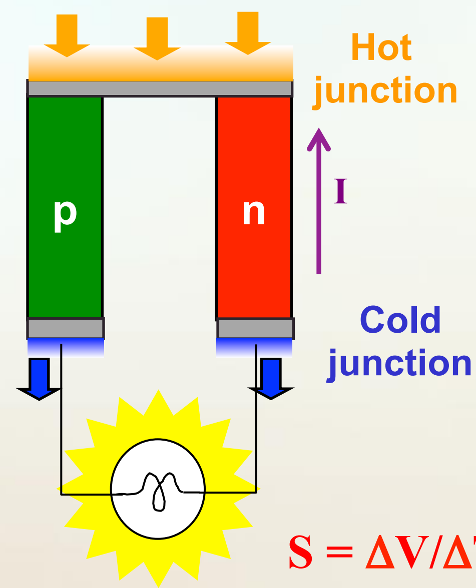

$S = \Delta V/\Delta T$

Power generation

TE Modules

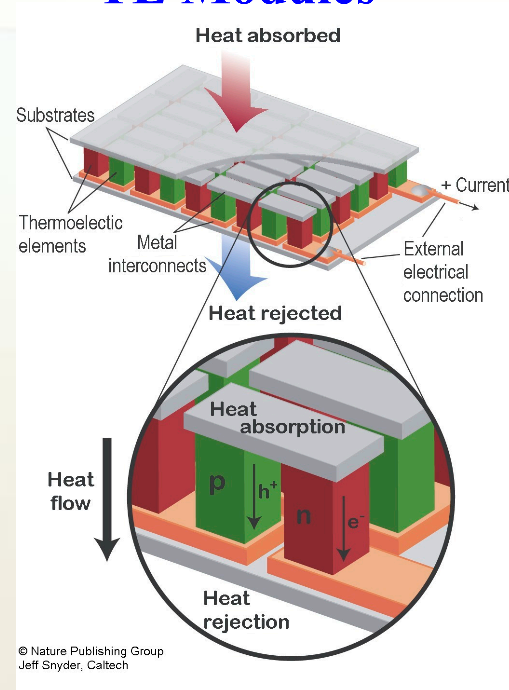

Applications : RTG* into space probes (Galieo and Ulysse)

Applications : Refrigerators (electronic systems)

* Radio-isotope Thermoelectric Generators

Thermoelectric Materials

- **TE oxides efficiency, ZT**

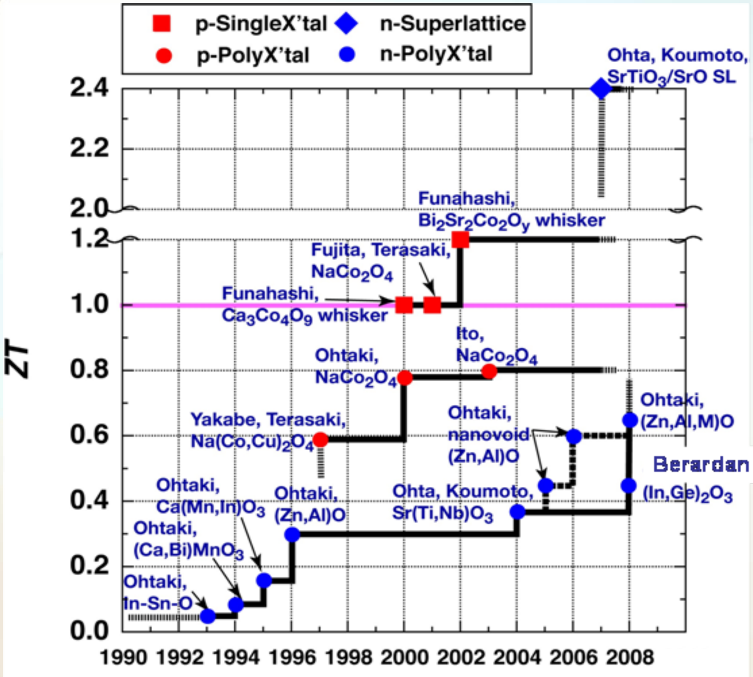

[Ohtaki-2008]

→ The figure-of-merite: ZT

$$ZT = \frac{S^2}{\rho . \kappa} T$$

[F.J. DiSalvo–1999]

S: Seebeck coefficient ($V.K^{-1}$)
T: Temperature (K)
ρ: Electrical resistivity (Ω.m)
κ: Thermal conductivity ($\Omega.m^{-1}.K^{-1}$)

$\kappa = \kappa_e + \kappa_{ph}$
- K_e: electronic contribution
- K_{ph}: phonon contribution

- **Why the $Ca_3Co_4O_9$ oxydes (349) ?**

✓ High thermal and chemical stabilities

✓ High oxidation resistance

✓ No toxic elements

Goal

- Master the 349 ceramics microstructure through Spark Plasma Sintering - SPS process

➡ Improve the mechanical and thermoelectric properties and correlate with the microstructure

➡ Integrate the performing 349 ceramics in thermoelectric modules

Elaboration of $Ca_3Co_4O_9$ ceramics

- $Ca_3Co_4O_9$ synthesised by solid-state method from CaCO3 and Co3O4 powders

- Spark Plasma Sintering (SPS): new processing technique (since 2000)

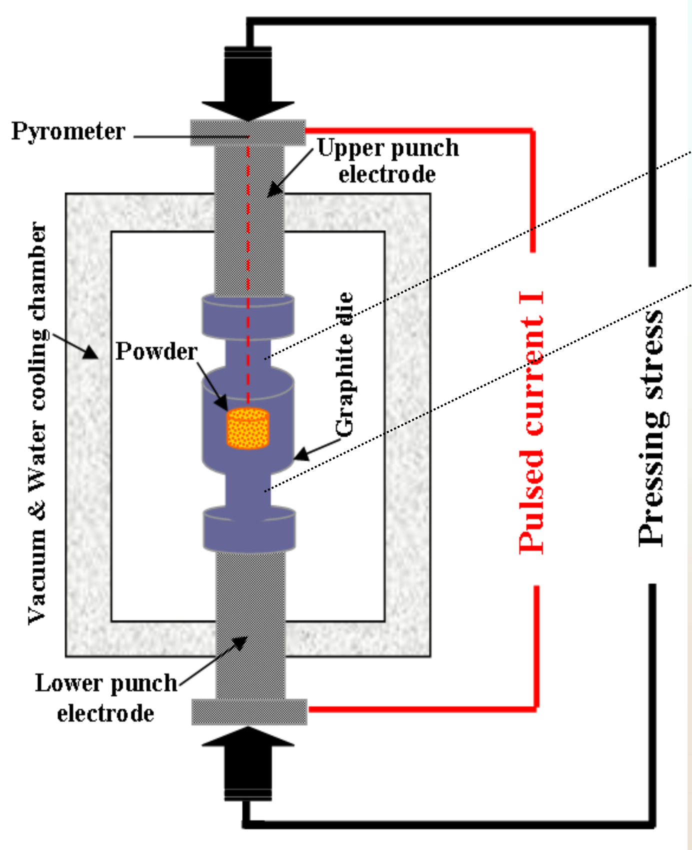

[M. Tokita-1999]

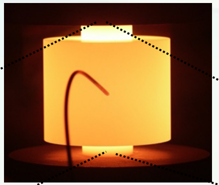

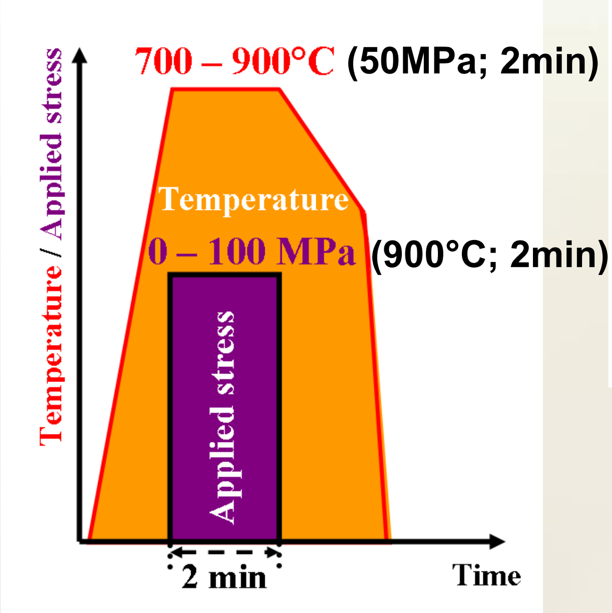

SPS System / FCT HP D25/I

MATEIS- INSA, Lyon, FRANCE

Microstructure and Texture

- **Pressing stress effects (0 - 100 MPa)**

Conventional sintering (0 MPa; 920°C; 24 h)

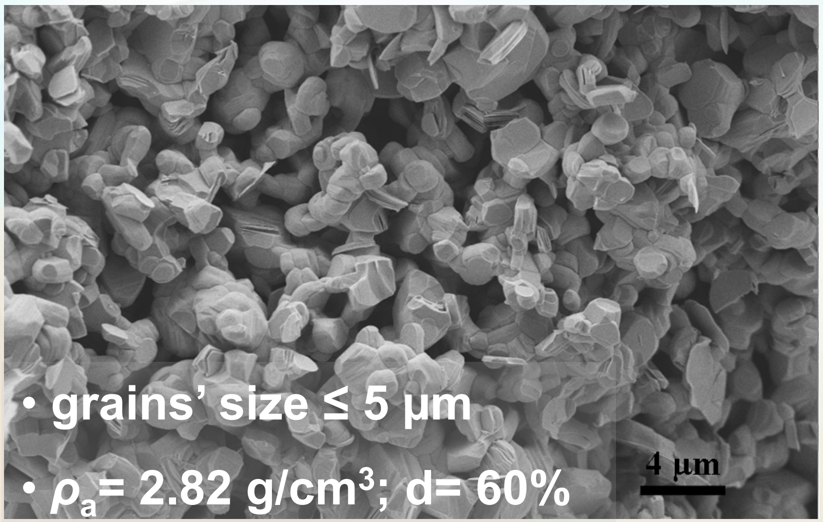

- grains' size ≤ 5 µm
- ρ_a= 2.82 g/cm^3; d= 60%

- Grains randomly oriented
- High porosity → Weak density

(Theoretical density : 4.68 g/cm^3) [Masset - 2000]

➤ **Pole Figures**

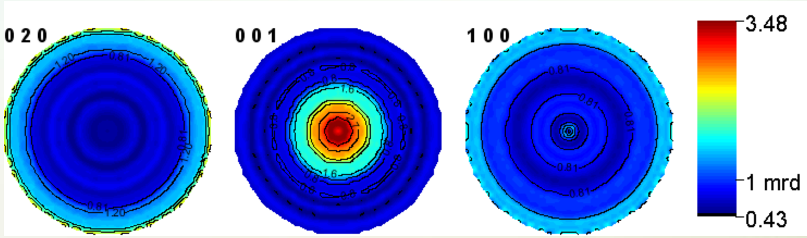

- The maximum of the {001} poles is 3.5 mrd. (multiples of a random distribution)

➡ This sample does not exhibit texture

Microstructure and Texture

Pressing stress
30 MPa
(900°C;2min)

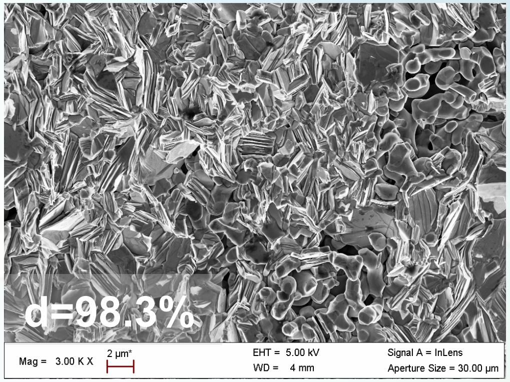

- **The maximum of the {001} poles is 3.74 mrd.**

50 MPa
(900°C;2min)

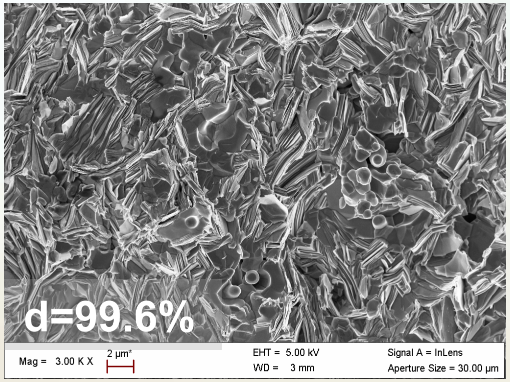

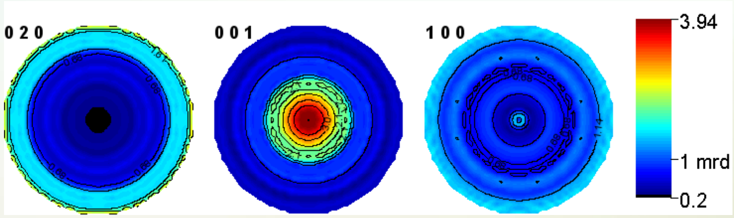

- **The maximum of the {001} poles is 3.94 mrd.**

75 MPa
(900°C;2min)

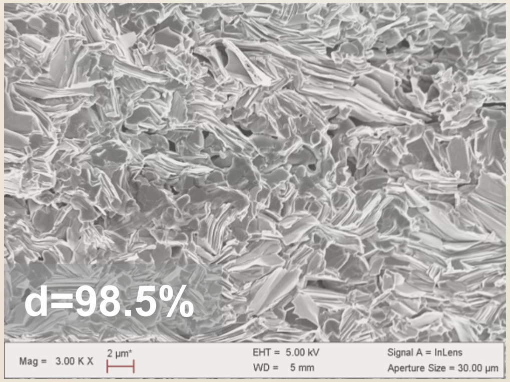

- **The maximum of the {001} poles is 4.05 mrd.**

Microstructure and Texture

- Temperature effects (700 – 900°C)

SPS Temperature

700°C

(50 MPa; 2 min)

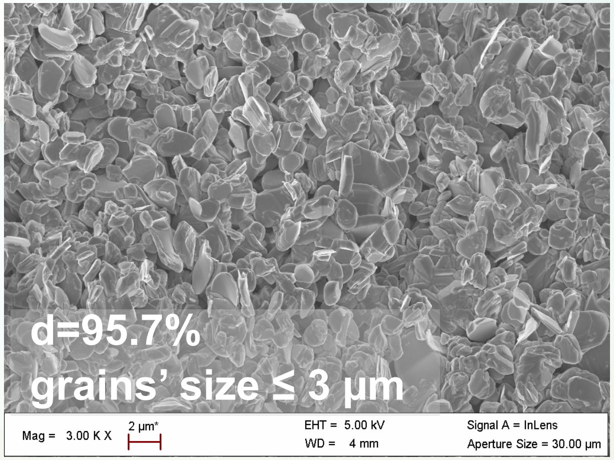

- The maximum of the {001} poles is 2.29 mrd.

850°C

(50 MPa; 2 min)

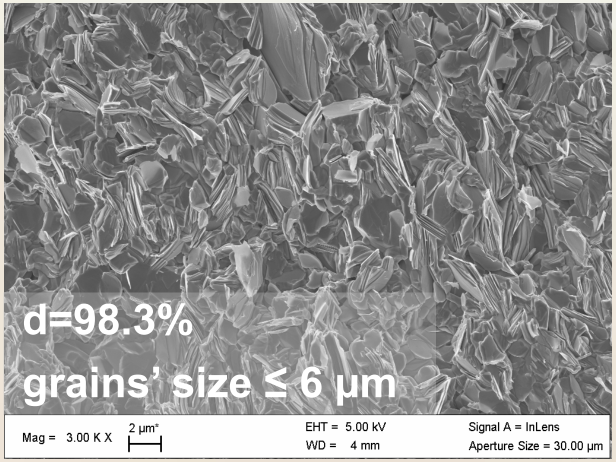

- The maximum of the {001} poles is 4.41 mrd.

Microstructure and Texture

➤ **Bulk density and maximum of {001} poles values for different applied stress levels and temperatures**

SPS stress (MPa)	0	30	50	75	100
Bulk density (%)	60	98.3	99.6	98.5	99.4
Maximum of {001} poles (m.r.d)	3.5	3.74	3.94	4.05	3.49

SPS temperature (°C)	700	750	800	850	900
Bulk density (%)	95.7	96.2	97.2	98.3	99.6
Maximum of {001} poles (m.r.d)	2.29	2.4	3.14	3.41	3.94

SPS pressing stress and temperature : 50 MPa; 900°C

Thermoelectric characterization

■ Pressing stress effects (0 - 100 MPa)

➤ Resistivity and Seebeck coefficient measurements

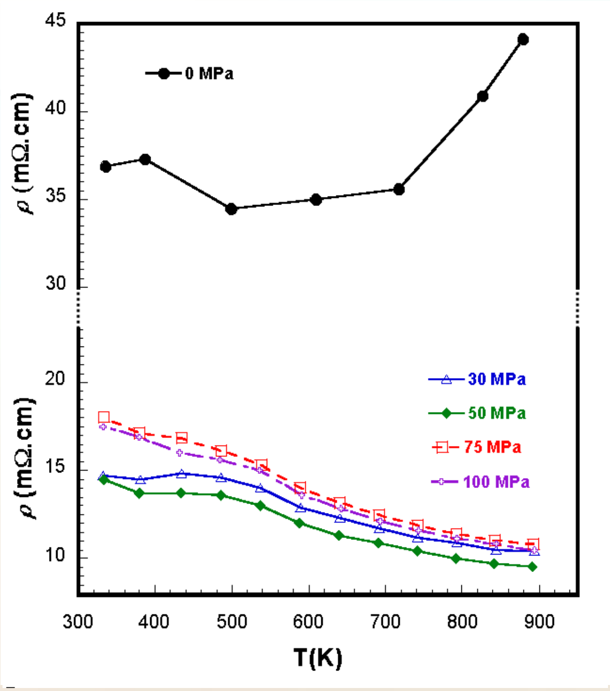

❑ ρ reduces with the pressing stress up to 50 MPa

- due to the increase in the bulk density.

❑ ρ increases for stress superior to 50 MPa

- due to the 'reappearance' of the weak zones at higher stress.

❑ Seebeck coefficient is independent of the pressing stress levels (as it is expected for)

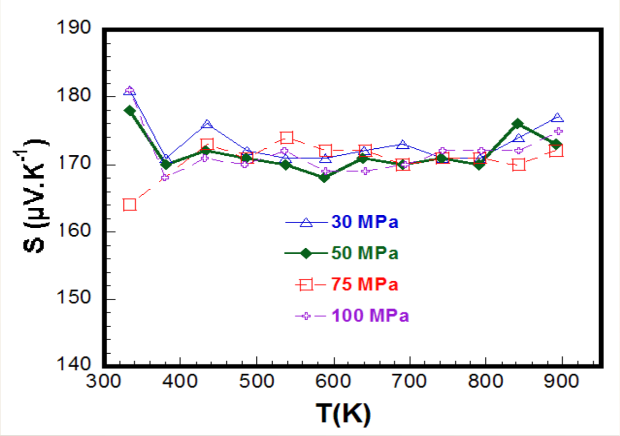

[Y. Zhang et al – 2003]

Thermoelectric characterization

- **Power factor,** $PF = \frac{S^2}{\rho}$

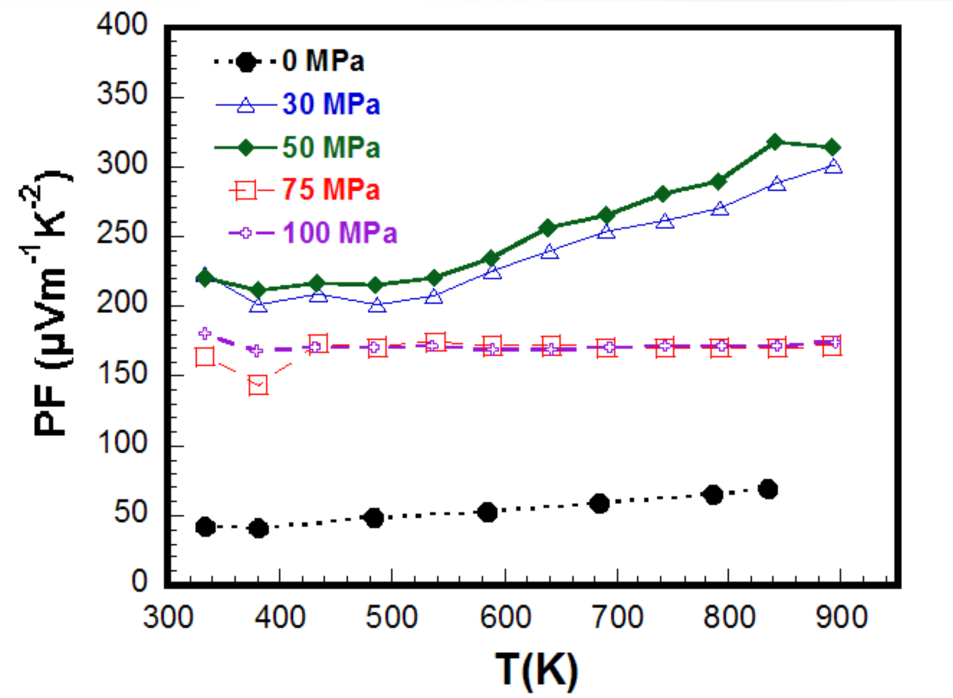

- **PF improves as the applied stress is increased up to 50 MPa**
- **Better PF values are obtained for SPS stress of 50 MPa**

[Y. Zhou et al – 2003]
[Y. Liu et al. 2005]

Better TE properties are found for 50 MPa

Thermoelectric characterization

- **Temperature effect (700 – 900°C)**

➤ **Resistivity and Seebeck coefficient measurements**

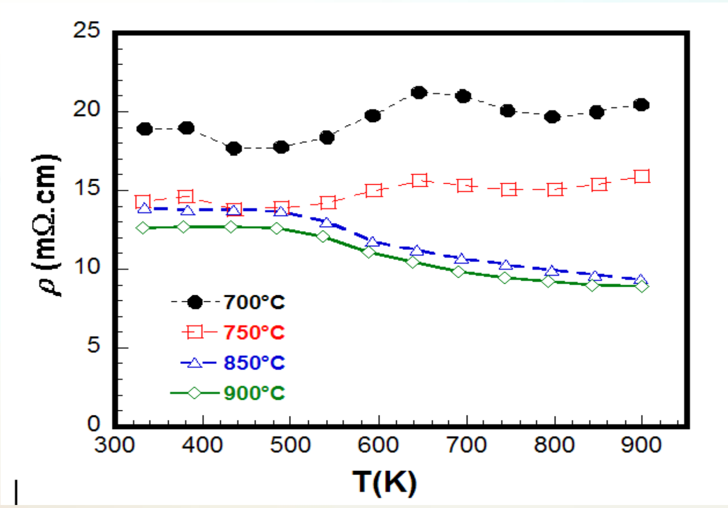

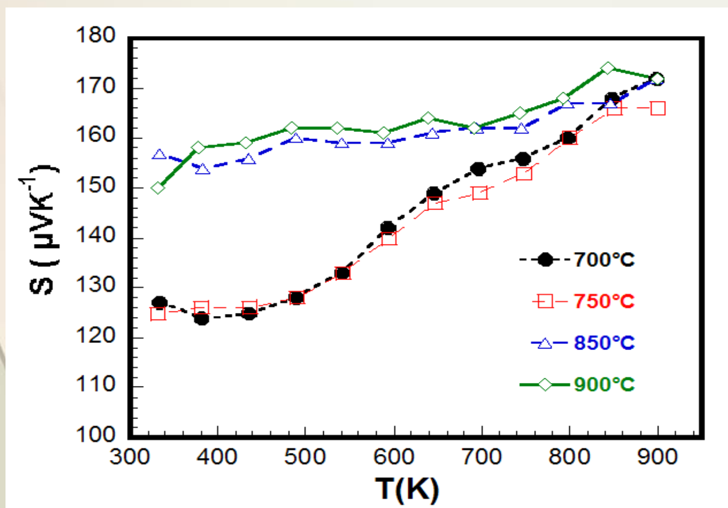

❑ **ρ reduces with the SPS temperature**

- due to the enhancement in the bulk density

❑ **Most reduced ρ values are obtained for 900°C**

❑ **Seebeck coefficient values are lower for temperatures of 700 and 750°C compared to those of 850 and 900°C.**

- Due to de difference in chemical composition

Thermoelectric characterization

- **Power factor,** $PF = \frac{S^2}{\rho}$

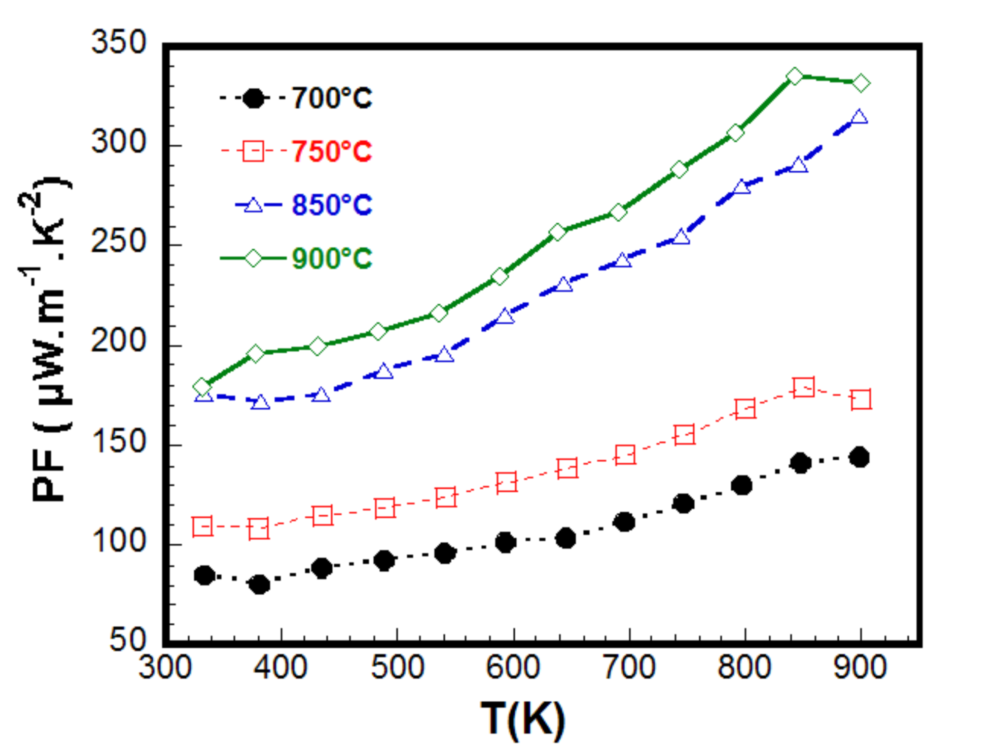

- **PF improves with the dwell temperature**

- **PF reaches 315 $\mu W.m^{-1}.K^{-2}$ at 840 K for a sample processed at 900°C.** **[Y. Zhou et al – 2003] [Y. Liu et al. 2005]**

Better TE properties are obtained for 50 MPa and 900°C

Mechanical properties

- **Nanoindentation (Indenter XP MTS)**

  - **Principle**

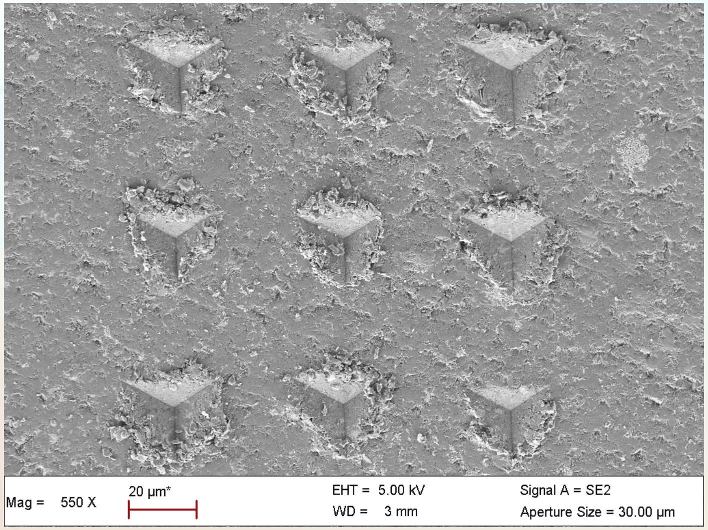

Pattern of residual impressions

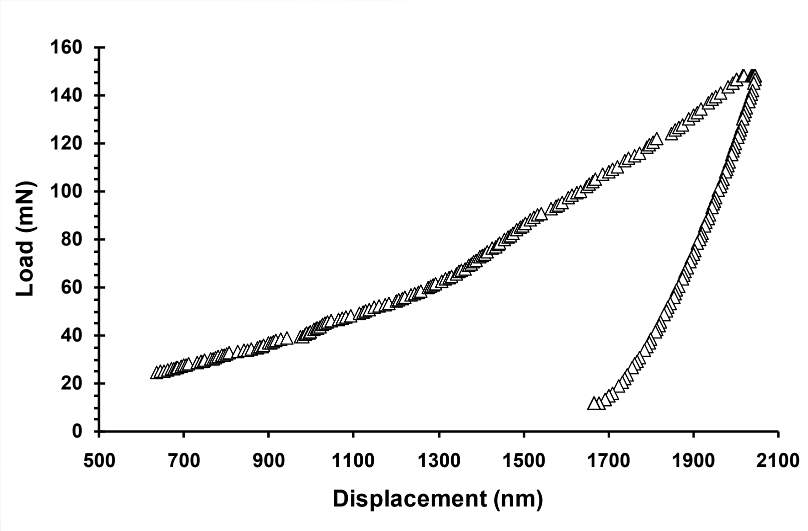

Load-displacement curve

Mechanical properties

- **Young's modulus, E**

$$E = (1-v^2)\ [1/E_r - (1-v_i^2) / E_i\ ]^{-1}$$

$E_r = (\pi 1/2.S)/(2.\beta.A1/2)$: the reduced modulus

S= dP/dh : the elastic stiffness; β = 1.0615

v and v_i are the Poisson's ratios of the specimen and indenter, respectively.

E_i : the elastic modulus of the indenter.

- **Hardness, H**

$$H = P_{max}/A$$

P_{max} : the load at the maximum penetration depth

A : the projected contact area between the indenter and the sample at P_{max}.

[W.C. Oliver – 1992]

[J. Woirgard – 1997]

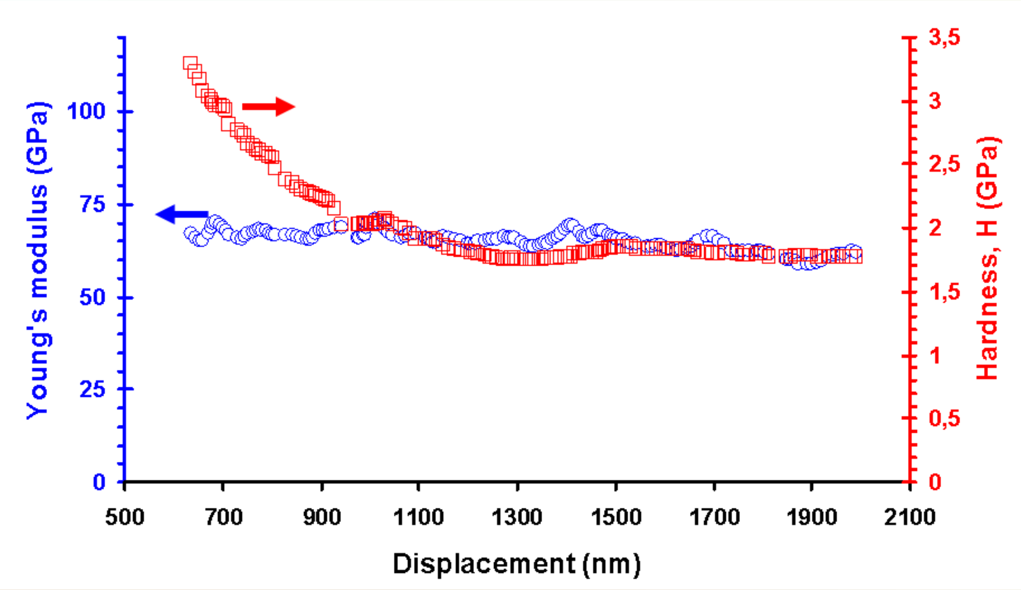

Hardness and Young's modulus versus displacement

Mechanical properties

- **Three point bending test**

➤ **The strength, σ_R**

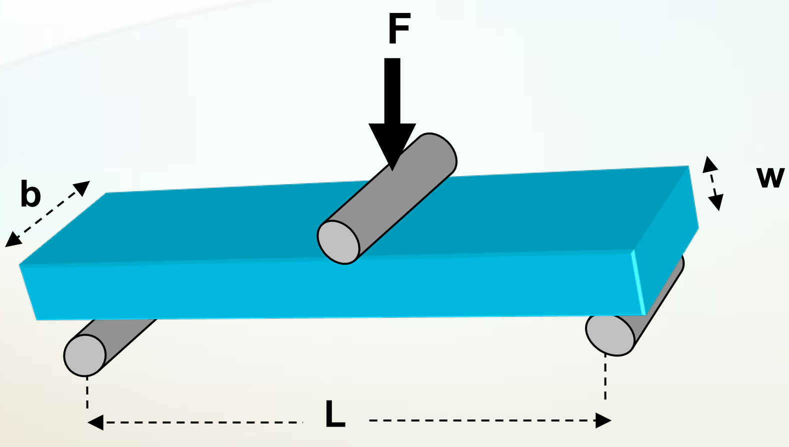

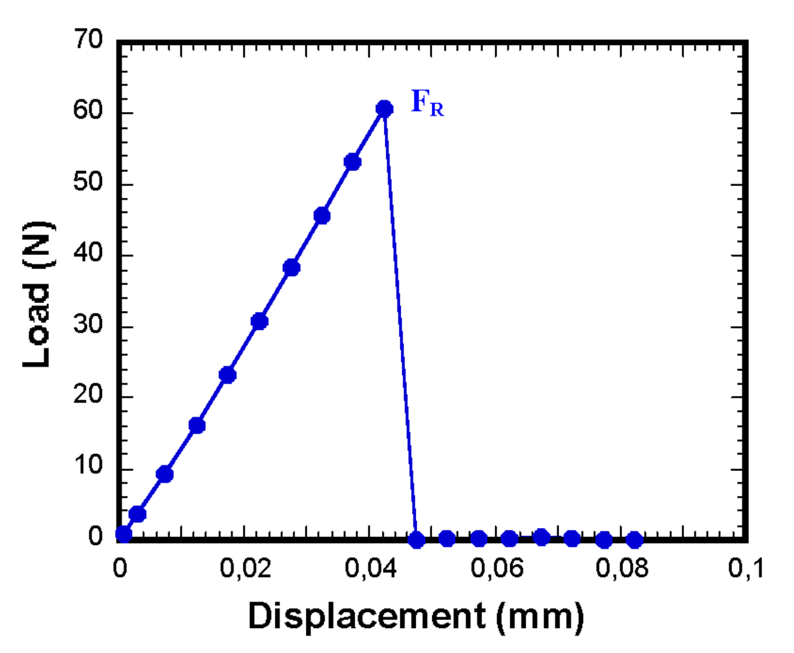

Load vs displacement for the sample processed under 50 MPa and at 900°C.

$$\sigma_R = \frac{3}{2}\frac{F_R L}{b w^2}$$

(F_R: Fracture load)

Mechanical properties

■ **Pressing stress effects (0 - 100 MPa)**

➤ **Hardness (H), Young Modulus (E), and Strength (σ_R), versus SPS pressing stress**

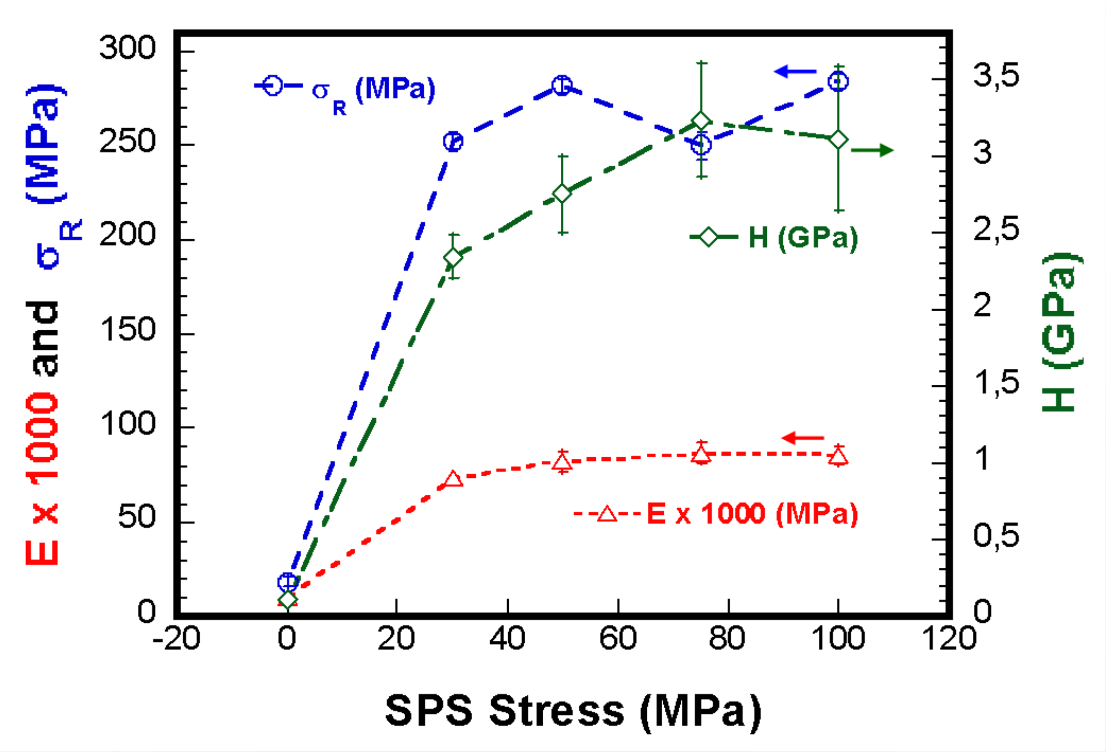

❑ **Considerable improvement of H, E and σ_R with the applied stress.**

→Due to the enhancement in the bulk density

❑ **A slower increase in H, E and σ_R at larger applied stress**

→ **Above 50 MPa, H, E and et σ_R are improved more than 29, 8, and 15 times, respectively, compared to the reference sample.**

Mechanical properties

- **Temperature effects (700 – 900°C)**

➤ **Hardness, H, Young Modulus, E, and Strength, σ_R, versus SPS temperature.**

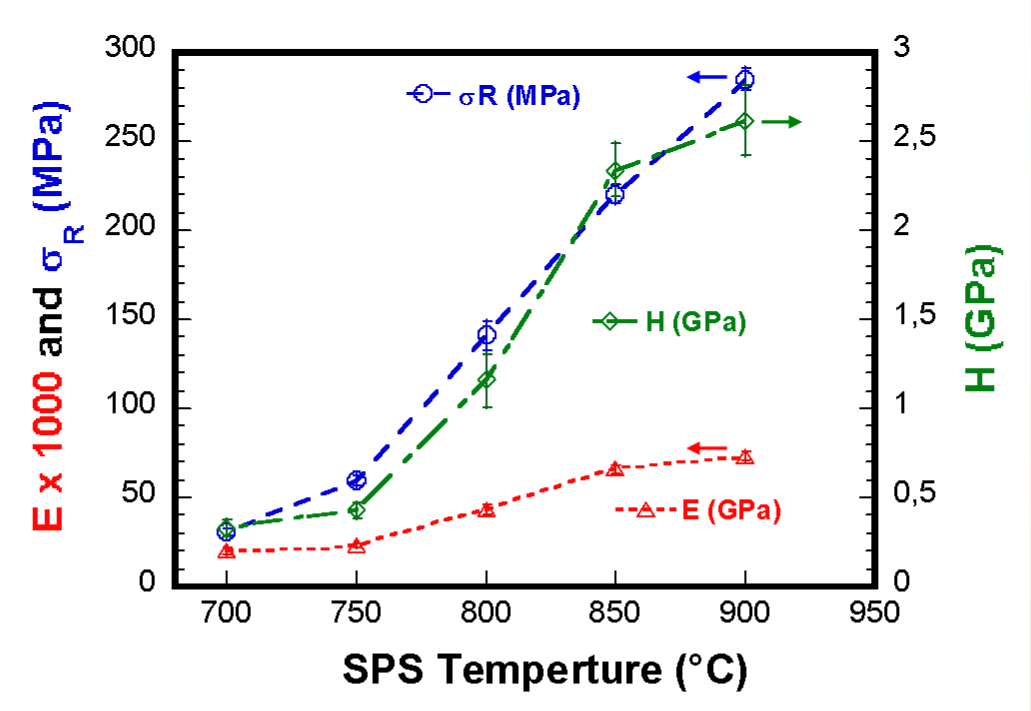

❑ **Improvement of H, E and σ_R with the SPS temperature.**

Due to :

- the enhancement in the bulk density,

- The chemical composition ??

→ Highest H, E and σ_R values are obtained for 900°C.

→ At 900°C, H, E and σ_R recorded an enhancement of 8, 3.5 and 9 times, respectively, compared to 700°C.

Conclusions

- The SPS process was used to consolidated the 349 TE ceramics

➡ The optimal thermomechanical cycle is :

50 MPa / 900°C / 2 min

➡ Rapid elaboration of 349 ceramics highly densified (99.7%)

➡ Enhancement of the thermoelectric performances

- PF at 840 K is increased from 70 (reference sample) to 315 $\mu W.m^{-1}.K^{-2}$

➡ Strong improvement of the mechanical properties

- H, E and et σ_R are improved more than 29, 8 and 15 times, respectively, compared to the reference sample

Current and future work

- Use new configurations at 900°C and 50 MPa in SPS to allow more texturation, grains size increase and densification

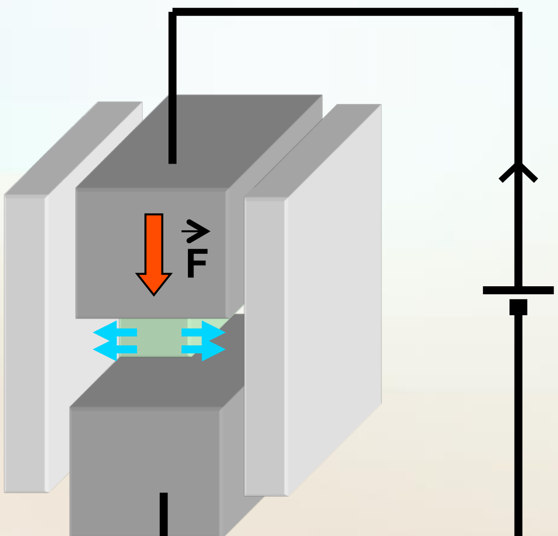

Starting material: Pre-sintered pellet
Free deformation configuration

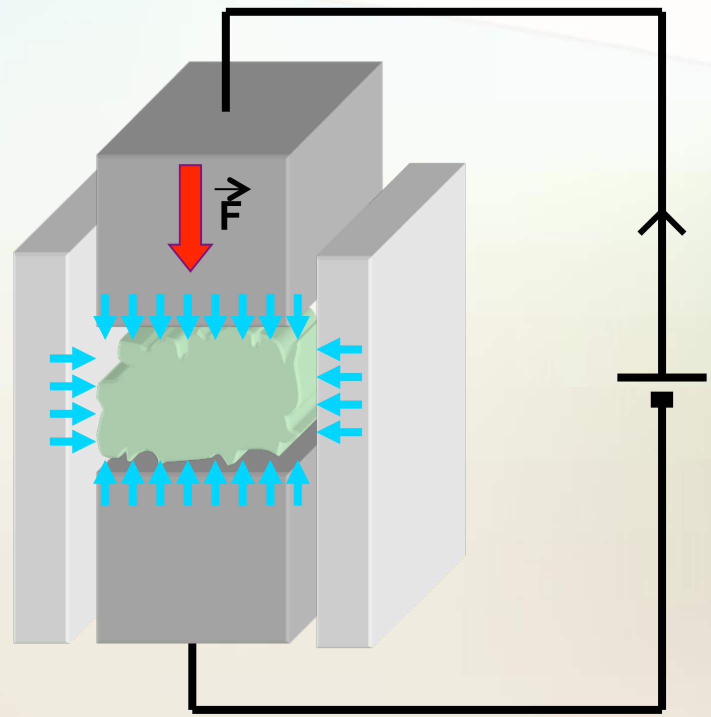

Starting material: Powder
Conventional SPS

Current and future work

- Fracture toughness tests
- Thermal conductivity measurements → ZT

➡ **Integration of 349 ceramics in thermoelectric modules**

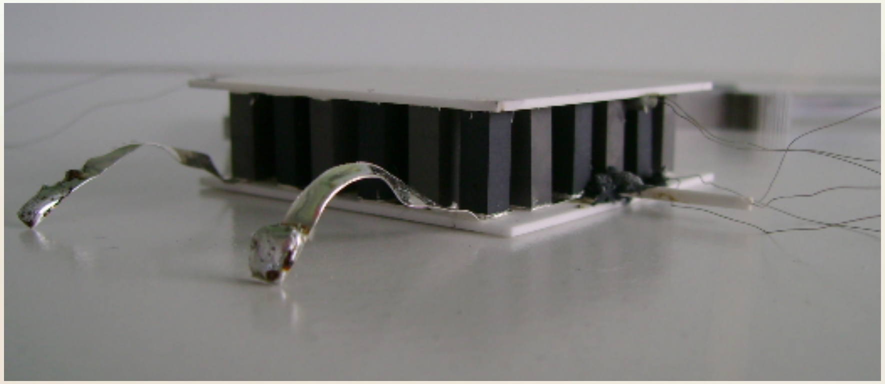

[*S. LEMONNIER – 2008*]

End.

Thank you for your attention!

$[Ca_2CoO_3]^{RS}[CoO_2]_{b1/b2}$

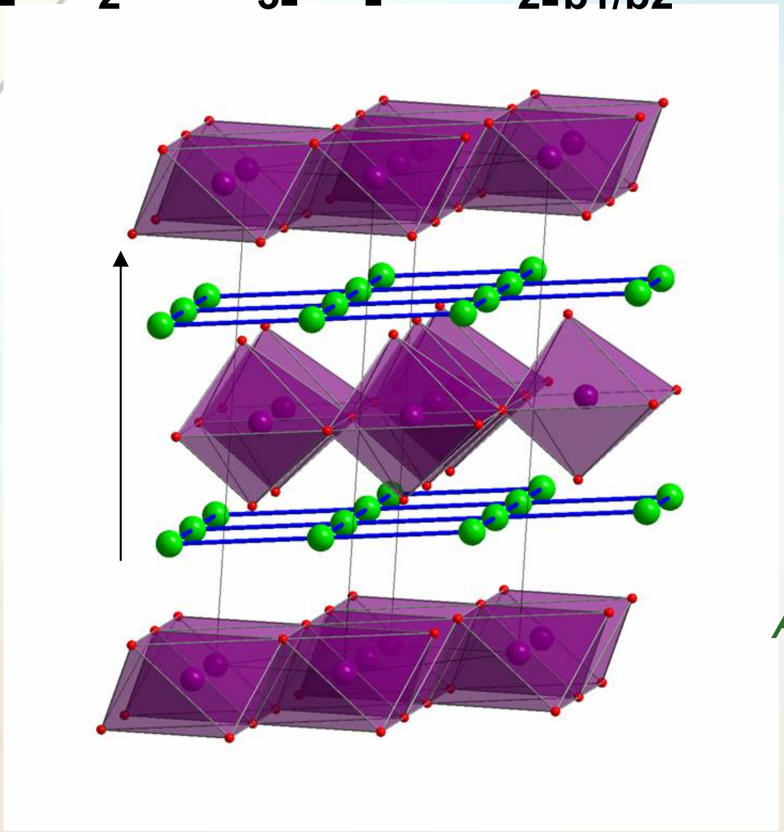

$CoO_2 = S_2$ (type CdI_2)

Responsable for conduction

CaO
CoO
CaO

$Ca_2CoO_3 = S_1$ (type NaCl = RS)

S1: a1=4,838

б1=4,557

c1=10,833

S2: a2=a1

б2=2,819,

c2=c1

A.C. Masset et al., Phys. Rev. B, 62-2000

$Ca_3Co_4O_9$: Misfit-layer structure with hexagonal CoO_2 layers, related to the CdI_2 type, and square Ca_2CoO_3 layers related to the NaCl type.
The Ca_2CoO_3 layers between the CoO_2 layers result in highly distorted interface and b-axis lattice misfit.

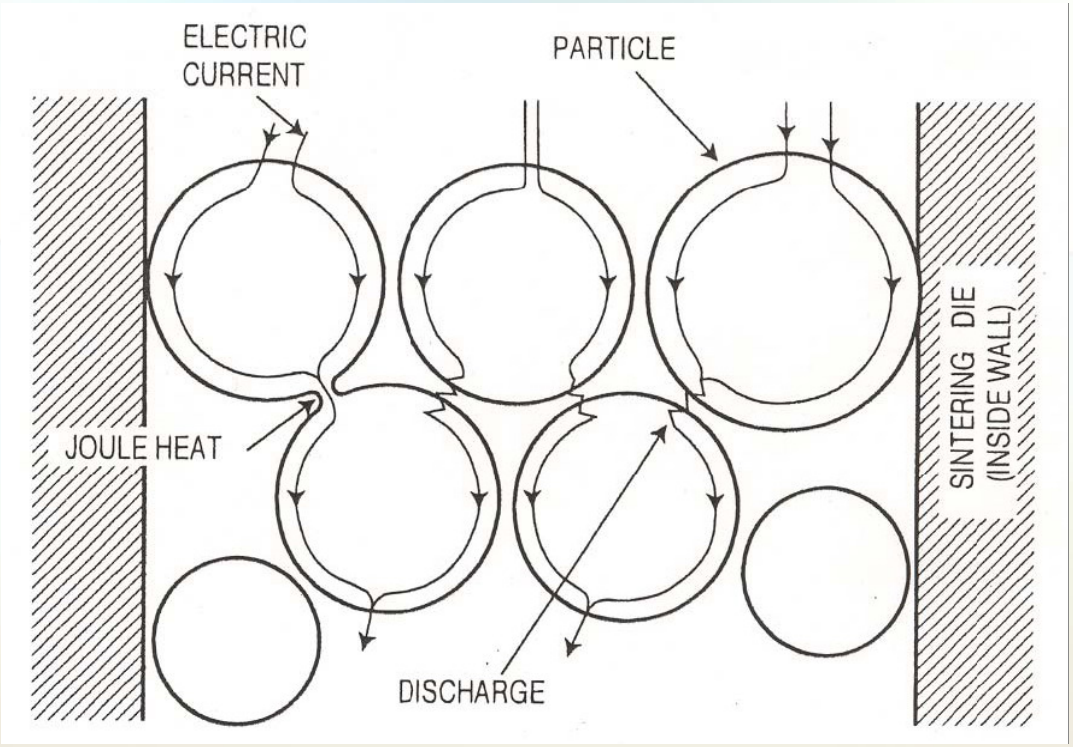

Illustration of how pulse current flows through powder particles inside the SPS sintering die

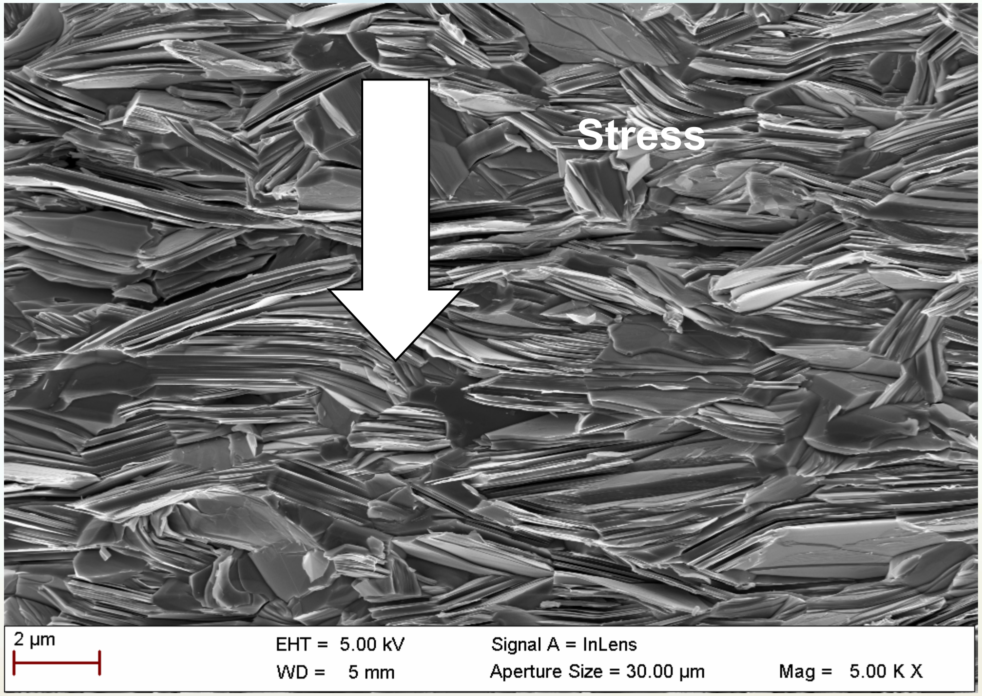

SPS-pellet,
900°C/2' /50 MPa